Polymorphs and stoichiometric variants of crown ether-based molecular complexes. Exploring the landscape of conformational flexibility and supramolecular interactions

Cinu Winson,[a] Saravanan Kandasamy,[c] Indira S. Divya,[ab] Krzysztof Wozniak[c] and Sunil Varughese[ab]

Supporting Information

Experimental

The compounds such as crown ethers (DCH and CE), dithioxamide (DTX), dinitroaniline (DNA), and the perflourohalocarbons were procured from Aldrich, India and were used for crystallization without further purification. The solvents used for crystallization were of HPLC grade, and a slow evaporation mode of crystallization was adopted. In a typical synthesis of the multicomponent systems, the respective crown ether was milled along with dithioxamide or dinitroaniline in the presence/absence of the perflourohalocarbons. The milling was performed in a Labindia ball mill MM1100 for 15 minutes. The milled materials were crystallized from various solvents and solvent-mixtures.

Single crystal X-ray Diffraction: Fine single crystals were used for X-ray diffraction studies at 100 K and mounted on MiTeGen micro-mounts with paratone-N oil. The diffraction data were collected on an Agilent Technologies SuperNova Dual Source diffractometer with Cu K_α radiation (λ = 1.54184 Å) equipped with an HyPix-6000HE hybrid pixel two-dimensional detector. CrysAlis Pro software (CrysAlisPRO, Oxford Diffraction/Agilent Technologies UK Ltd, Yarnton, England) was used to process the data sets. In addition, the data sets were corrected for Lorenz and polarization effects. All crystal structures were solved by direct methods and subsequently refined with full-matrix least-squares on *F*2, applying SHELXL with the graphical interface of the Olex[2].

Hirshfeld surface analysis: Hirshfeld surface 2D fingerprint plot was constructed using Crystal Explorer (Ver. 17.5, University of Western Australia). The intermolecular interaction and energy frameworks were calculated at B3LYP/6-31G(d,p) level of dispersion-corrected density functional theory basis set. The energy framework was constructed based on the total intermolecular interaction energy, including electrostatic, polarization, dispersion and exchange-repulsion components.

Full Interaction Maps (FIMs): The FIMs analysis was performed using Mercury as the structure visualizer. The interaction maps of uncharged NH and OH of water were analyzed in the context of crystal packing. The interaction maps indicate hydrogen bond donors (blue) and acceptors (red), respectively.

Thermal Analysis: The thermal stability and decomposition profile of the crystalline compounds were measured using a Mettler TGA 2 thermogravimmetric analyzer, with a heating rate of 5 °C/min under a nitrogen atmosphere

Molecular Electrostatic Potential (MESP) Analysis: Theoretical calculations were carried out in Gaussian 16. We optimized the molecules and calculated their single-point energy with a DFT method at the level of B3LYP/6-311+G(d,p). Individual molecules were visualized in GaussView 6.0.

Conformational Studies: The molecular conformation and the point groups were analysed using VMD 1.9.4a53 software suite and the embedded Symmetry Tool.

Table S1 Crystallographic Information

Compound	DTX-I	DTX-II	DTX-III	DTX-IV	DNA-I	DNA-II	DNA-III
Formula	$C_{20}H_{36}O_6$, $2(C_2H_4N_2S_2)$	$C_{20}H_{36}O_6$, $2(C_2H_4N_2S_2)$	$C_{20}H_{36}O_6$, $2(CH_2NS)$, H_2O	$C_{20}H_{36}O_6$; $C_2H_4N_2S_2$	$C_{20}H_{36}O_6$; $2(C_6H_5N_3O_4)$	$C_{20}H_{36}O_6$; $2(C_6H_5N_3O_4)$	$C_{20}H_{36}O_6$; $2(C_6H_5N_3O_4)$,
Ratio	1:2	1:2	1:2(0.5):1	1:1	1:2	1:2	1:2
CCDC Nos.	AJUXIM	AJUXOS	2412481	2412480	2412478	2412479	2412482
Formula Wt.			510.720	492.705	738.754	738.75	492.705
Crystal habit			Acicular	Acicular	Block	Block	Block
Crystal colour			Red	Red	Yellow	Yellow	Yellow
Crystal system	Monoclinic	Monoclinic	Monoclinic	Triclinic	Monoclinic	Triclinic	Triclinic
Space group	$C2/c$	$P2_1/n$	$P2_1/c$	$P\bar{1}$	$P2_1/c$	$P\bar{1}$	$P\bar{1}$
***a* (Å)**	23.720(1)	12.654(3)	8.189(1)	10.1460(2)	7.5430(1)	8.3820(1)	11.5000(1)
***b*(Å)**	7.655(2)	7.5700(15)	14.730(1)	14.1440(3)	11.8220(1)	11.4920(2)	16.7610(2)
***c* (Å)**	18.364(3)	17.129(3)	21.856(2)	14.5050(3)	20.0720(2)	19.2230(3)	19.5890(2)
***α* (º)**	90	90	90	91.7000(19)	90	86.229(2)	104.953(1)
***β* (º)**	106.98(6)	106.14(3)	90.56(1)	105.5010(19)	99.410(1)	80.130(1)	91.171(1)
***γ* (º)**	90	90	90	101.171(2)	90	84.865(2)	95.137(1)
***V* (Å^3)**			2636.23(4)	1960.51(8)	1765.80(3)	1765.80(3)	3629.58(7)
Z	4	2	4	3	2	2	4
***D*calc(g cm^{-3})**			1.287	1.252	1.389	1.352	1.352
***T*(K)**			100(2)	100(2)	100(2)	100(2)	100(2)
(*λ*)Cu K*α*			1.54184	1.54184	1.54184	1.54184	1.54184
***μ*(mm^{-1})**			2.188	2.160	0.929	0.904	0.904
2*θ* range (º)			155.02	155.38	155.18	155.5	155.36
Total Reflns.			60133	47546	41039	42169	99456
Unique Reflns.			5565	8228	3752	7616	15273
Reflns. Used			5139	7384	3355	6603	13540
No. Parameters			324	456	235	485	944
GOF on *F*^{2}			1.0307	1.0237	1.0273	1.0473	1.0377
Final *R*1, *wR*2			0.0319, 0.0808	0.0416, 0.1125	0.0365, 0.0934	0.0600, 0.1544	0.0455, 0.1465

Table S1 Crystallographic Information (Contd…)

Compound	**CE-I**	**C6**	**T-I**
Formula	$C_{12}H_{24}O_6$, $C_2H_4N_2S_2$, $2(H_2O)$	$C_{12}H_{24}O_6$ $2(C_2H_4N_2S_2)$	$C_{20}H_{36}O_6$; $2(C_6H_5N_3O_4)$; $C_6F_4I_2$
Ratio	1:1:2H_2O	1:2	1:2:1
CCDC Nos.	2412475	2412476	2412477
Formula Wt.	420.551	504.720	1140.623
Crystal habit	Block	Block	Block
Crystal colour	Red	Yellow	Yellow
Crystal system	Triclinic	Monoclinic	Triclinic
Space group	$P\bar{1}$	$P2_1/n$	$P\bar{1}$
***a* (Å)**	7.3962(3)	8.5145(2)	10.5860(3)
***b*(Å)**	7.7483(3)	14.7946(3)	11.3120(4)
***c* (Å)**	10.1053(3)	10.0414(2)	11.3900(4)
***α* (°)**	74.404(3)	90	68.084(3)
***β* (°)**	72.510(3)	104.389(2)	66.508(3)
***γ* (°)**	75.828(3)	90	64.091(3)
***V* (Å^3)**	523.46(4)	1225.22(5)	1091.91(7)
Z	1	2	1
***D*calc(g cm^{-3})**	1.334	1.368	1.735
***T*(K)**	100(2)	100(2)	100(2)
(*λ*)Cu K*α*	1.54184	1.54184	1.54184
***μ*(mm^{-1})**	2.674	3.895	12.103
2*θ* range (°)	155.26	156.00	154.84
Total Reflns.	9294	25884	22539
Unique Reflns.	2186	2606	4573
Reflns. Used	2136	2442	4461
No. Parameters	126	143	306
GOF on *F*^{2}	1.0517	1.0475	1.0417
Final *R*1, *wR*2	0.0306, 0.0884	0.0313, 0.0861	0.0674, 0.1793

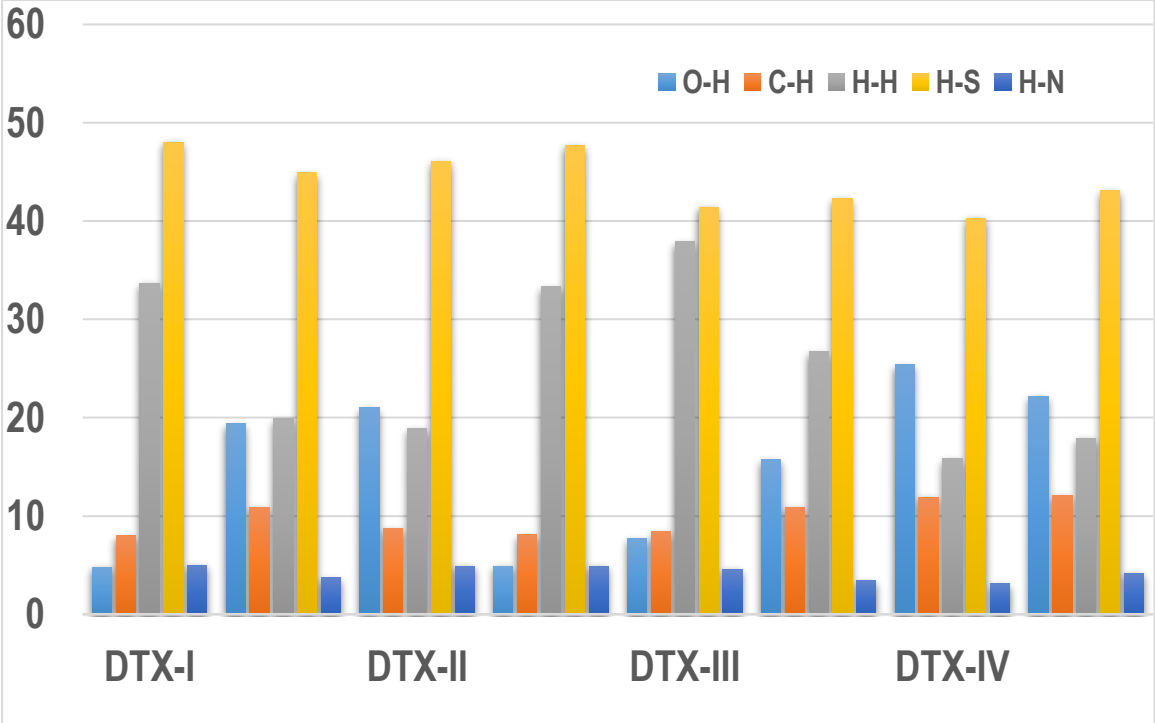

Fig. S1 Relative contribution of various interaction types in the complexes of DTX.

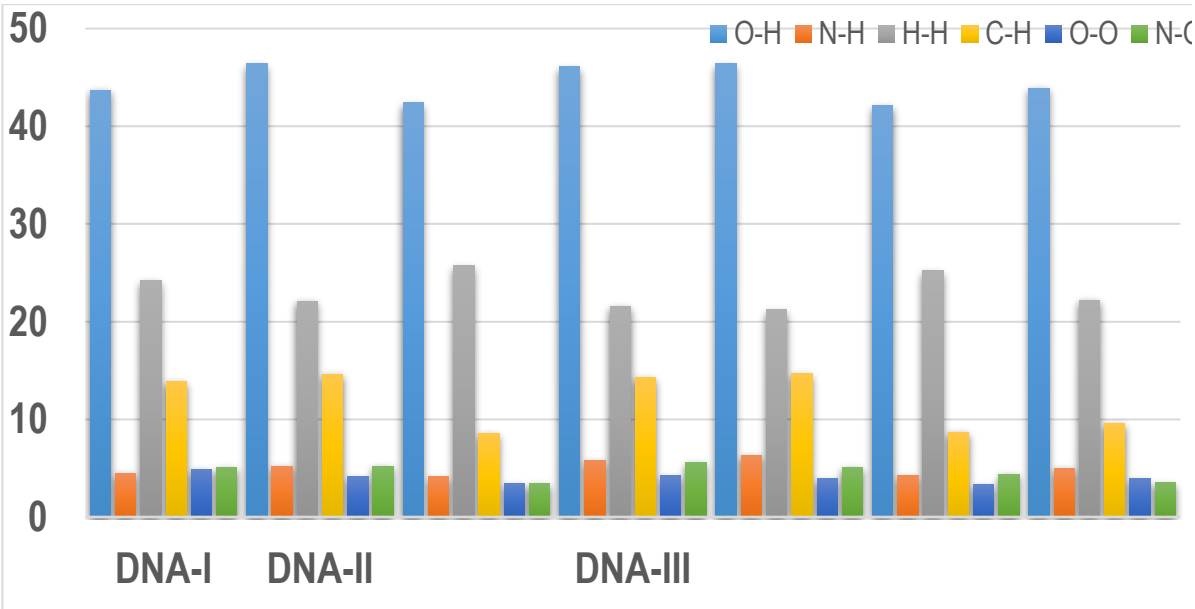

Fig. S2 Relative contribution of various interaction types in the complexes of DNA.

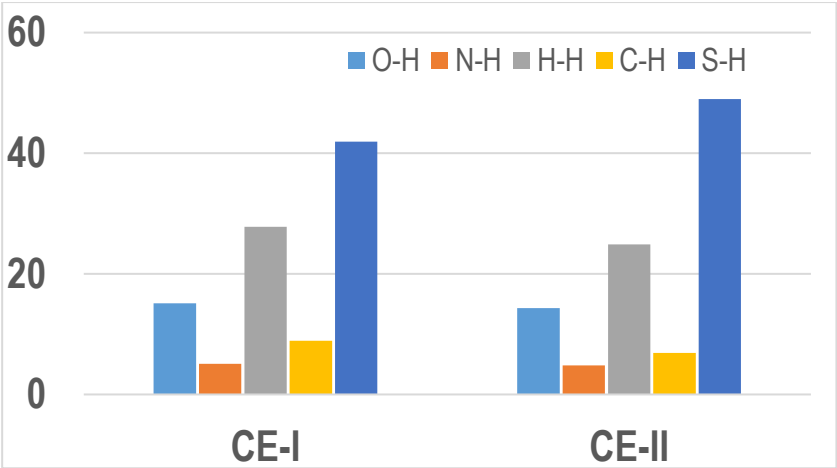

Fig. S3 Relative contribution of various interaction types in the complexes of CE.

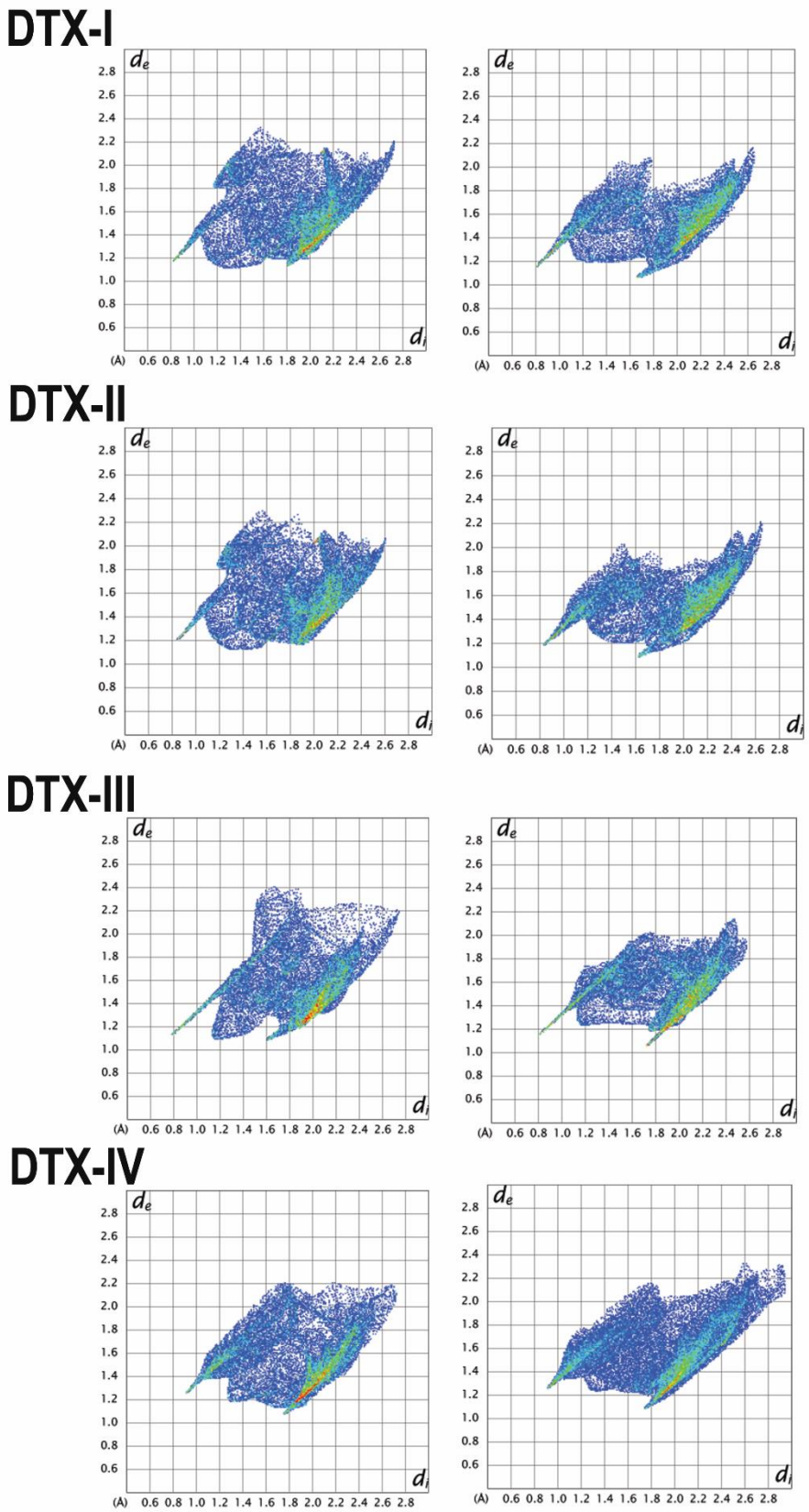

Fig. S4 Fingerprint plots of the DTX moieties in the complexes with DCH.

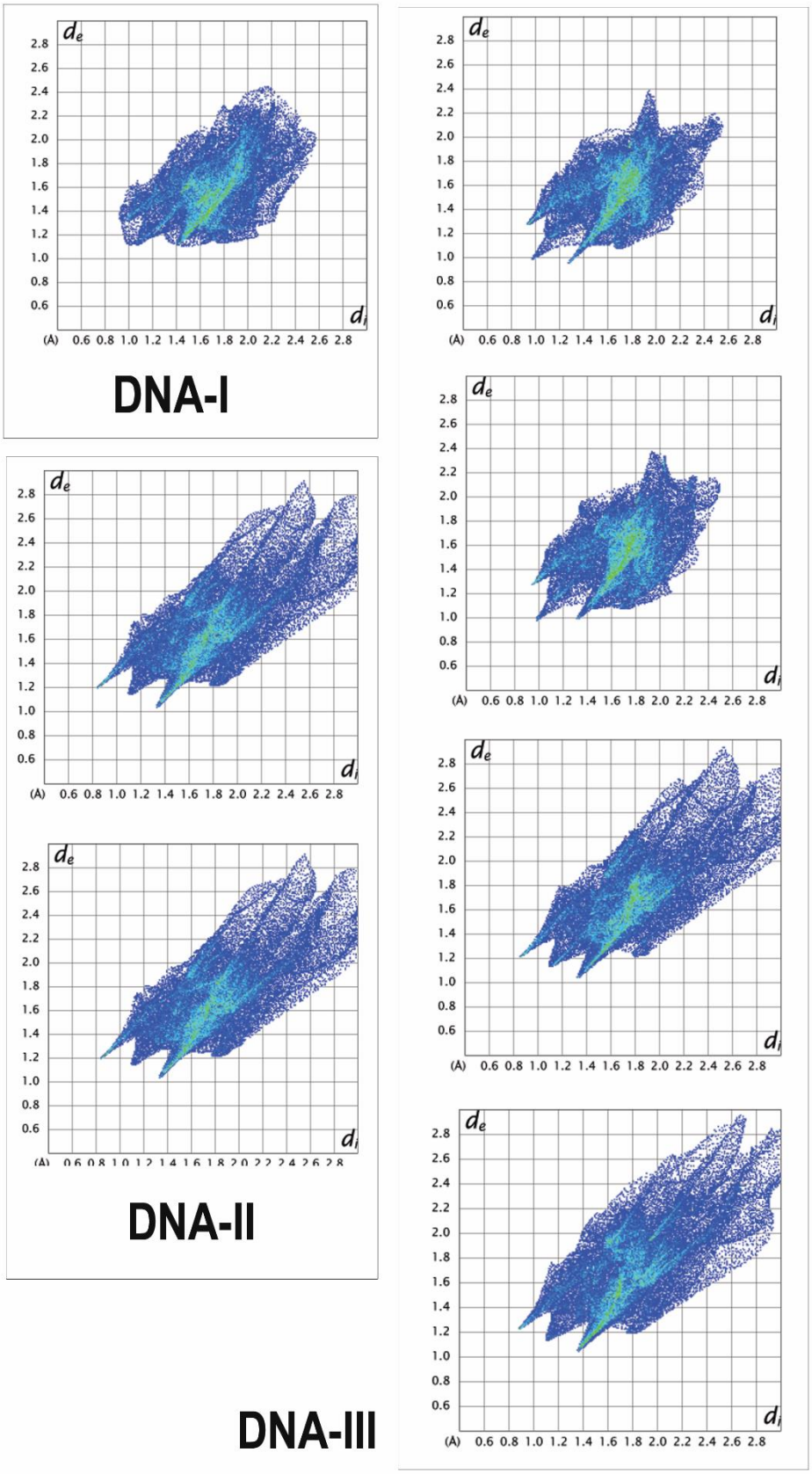

Fig. S5 Fingerprint plots of the DNA moiety in its complexes with DCH.

DTX-I

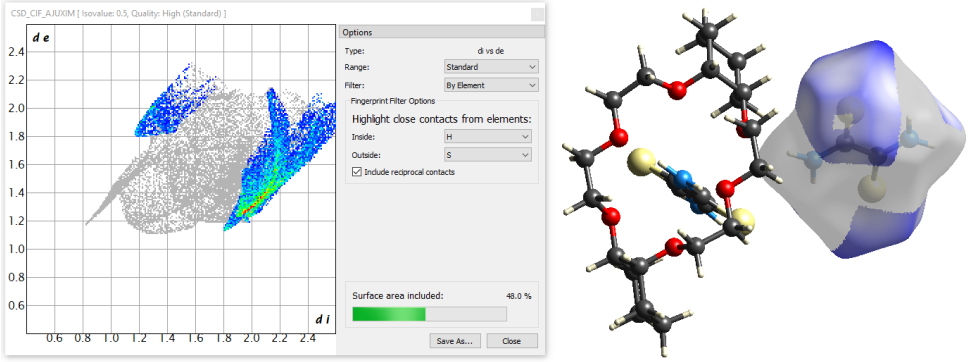

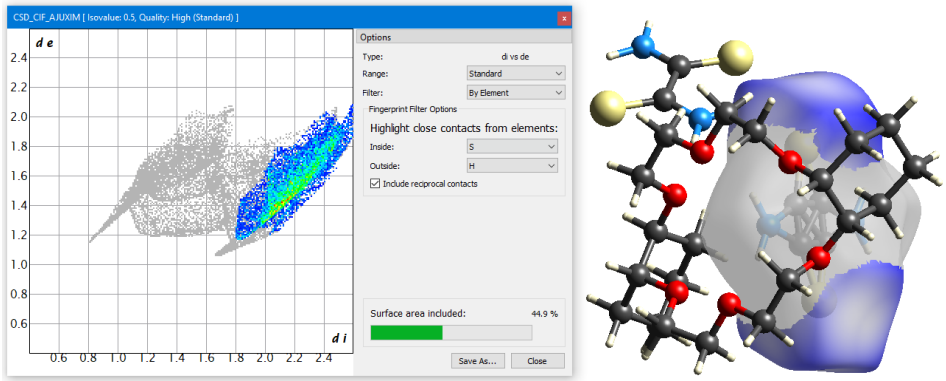

DTX-II

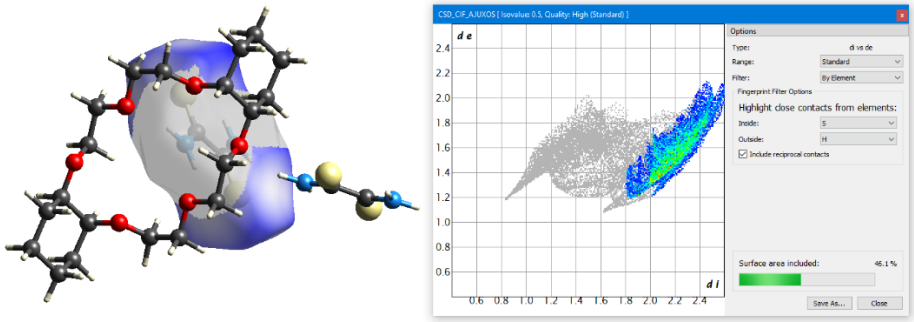

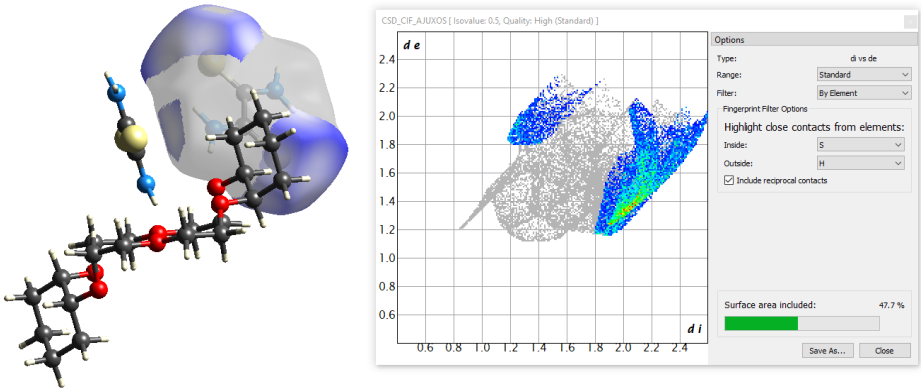

DTX-III

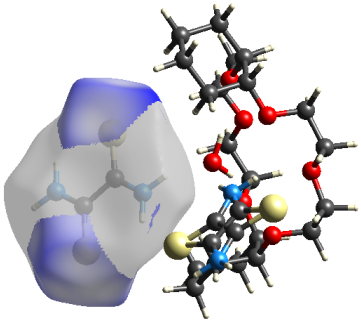

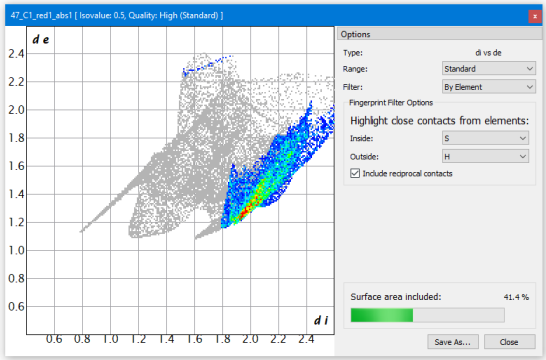

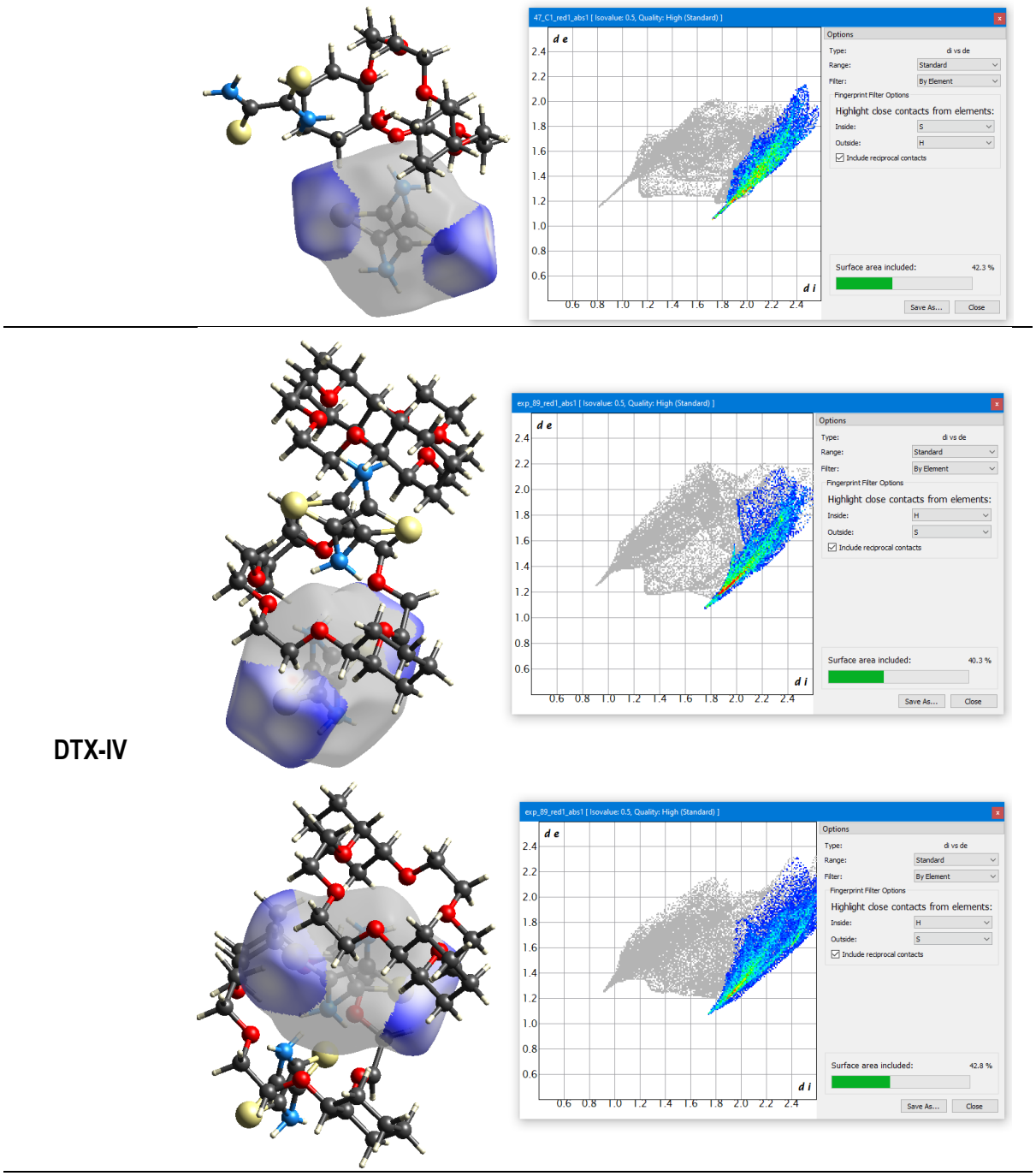

Fig. S6 The S⋯H interactions in the DTX complexes and the corresponding fingerprint plots

DNA-I

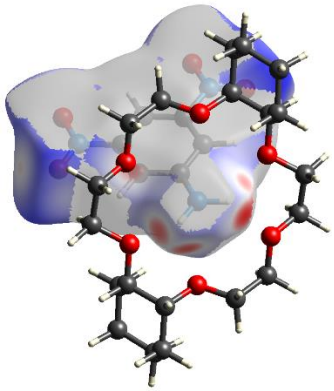

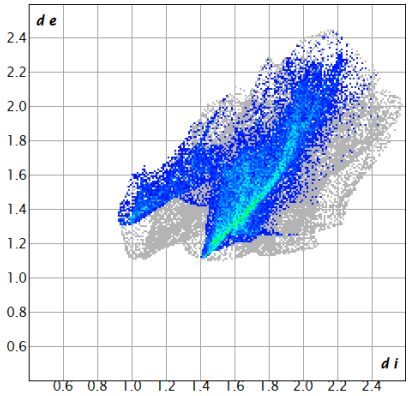
d e
2.4
2.2
2.0
1.8
1.6
1.4
1.2
1.0
0.8
0.6
d i
0.6 0.8 1.0 1.2 1.4 1.6 1.8 2.0 2.2 2.4

DNA-II

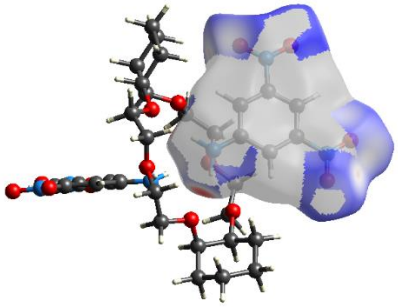

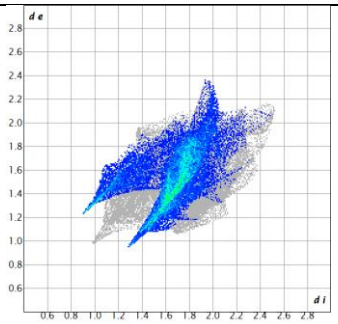
d e
2.8
2.6
2.4
2.2
2.0
1.8
1.6
1.4
1.2
1.0
0.8
0.6
d i
0.6 0.8 1.0 1.2 1.4 1.6 1.8 2.0 2.2 2.4 2.6 2.8

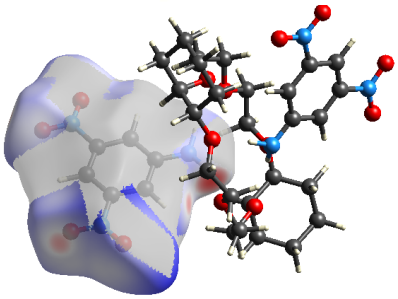

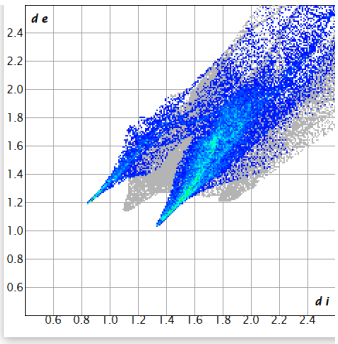
d e
2.4
2.2
2.0
1.8
1.6
1.4
1.2
1.0
0.8
0.6
d i
0.6 0.8 1.0 1.2 1.4 1.6 1.8 2.0 2.2 2.4

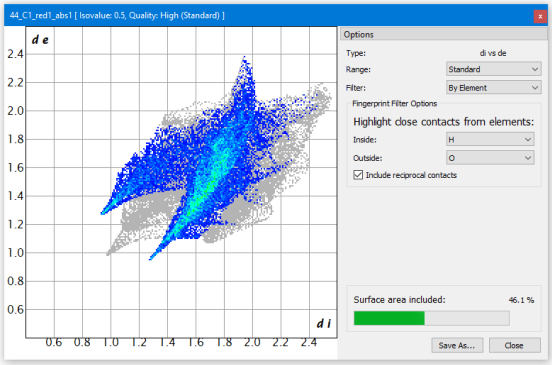
44_C1_red1_abs1 [Isovalue: 0.5, Quality: High (Standard)]
d e
2.4
2.2
2.0
1.8
1.6
1.4
1.2
1.0
0.8
0.6
d i
0.6 0.8 1.0 1.2 1.4 1.6 1.8 2.0 2.2 2.4
Options
Type: di vs de
Range: Standard
Filter: By Element
Fingerprint Filter Options
Highlight close contacts from elements:
Inside: H
Outside: O
Include reciprocal contacts
Surface area included: 46.1 %
Save As...
Close

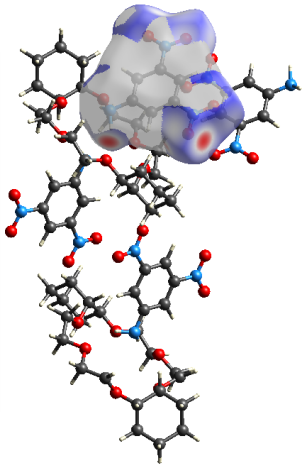

DNA-III

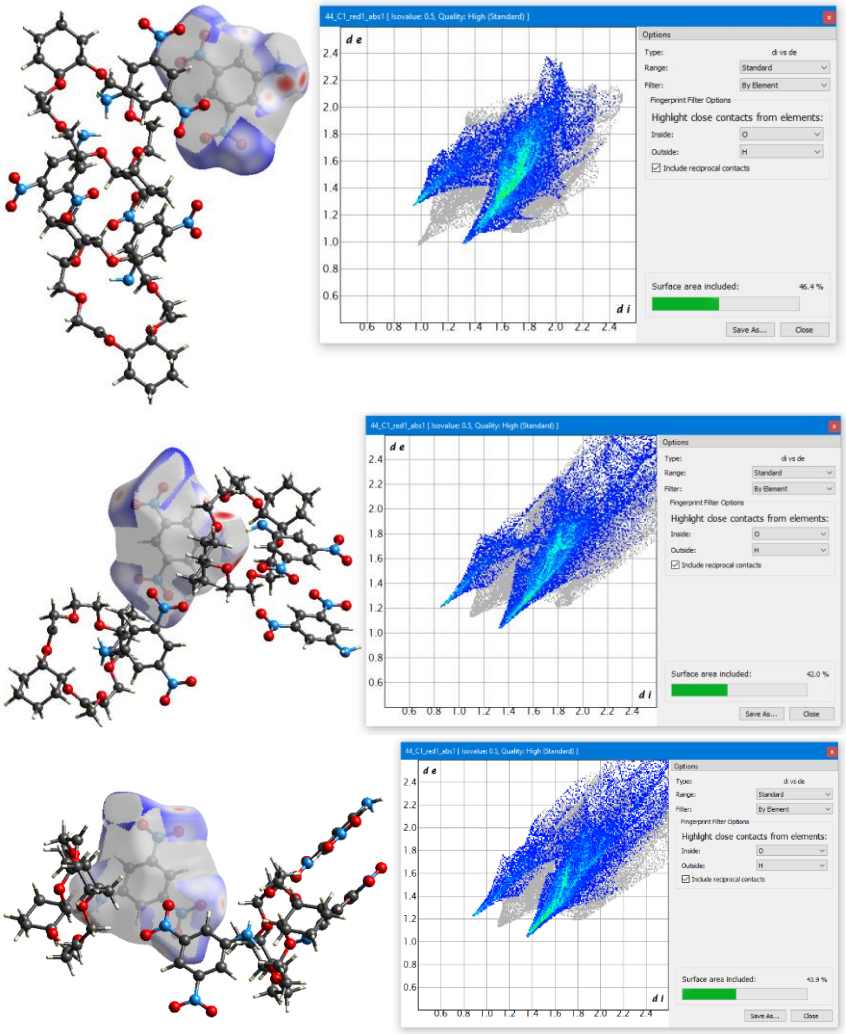

Fig. S6 The O⋯H interactions in the DNA complexes and the corresponding fingerprint plots

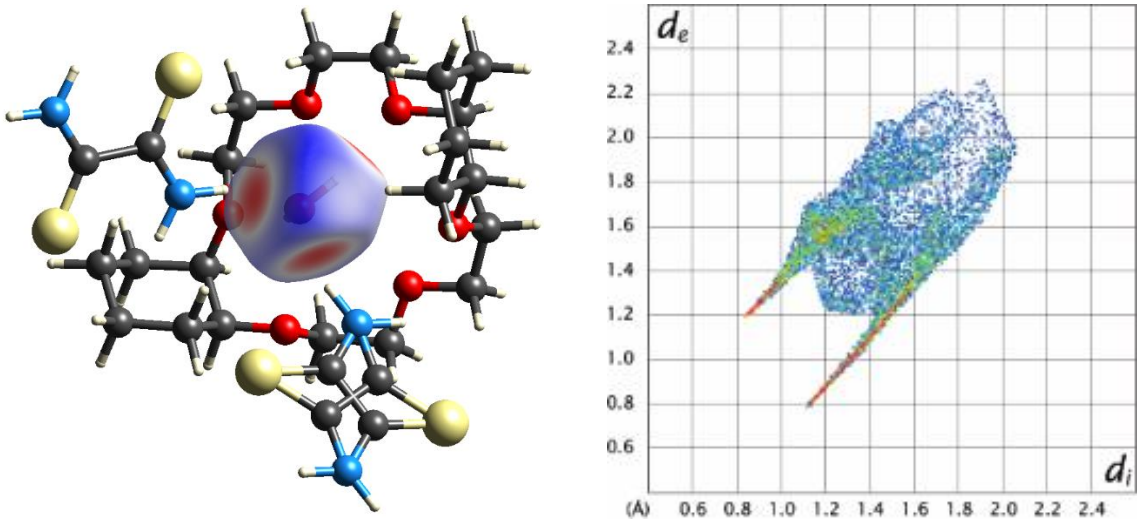

DTX-III

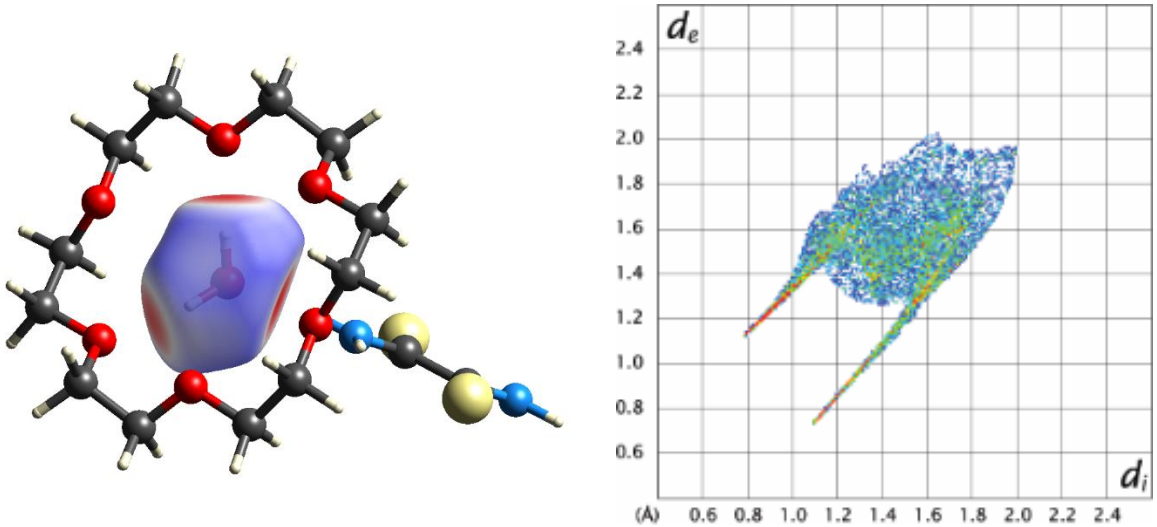

C6-I

Fig. S6 The ESP surface and the fingerprint plots of water in the hydrated systems (DTX-III and C6-1).

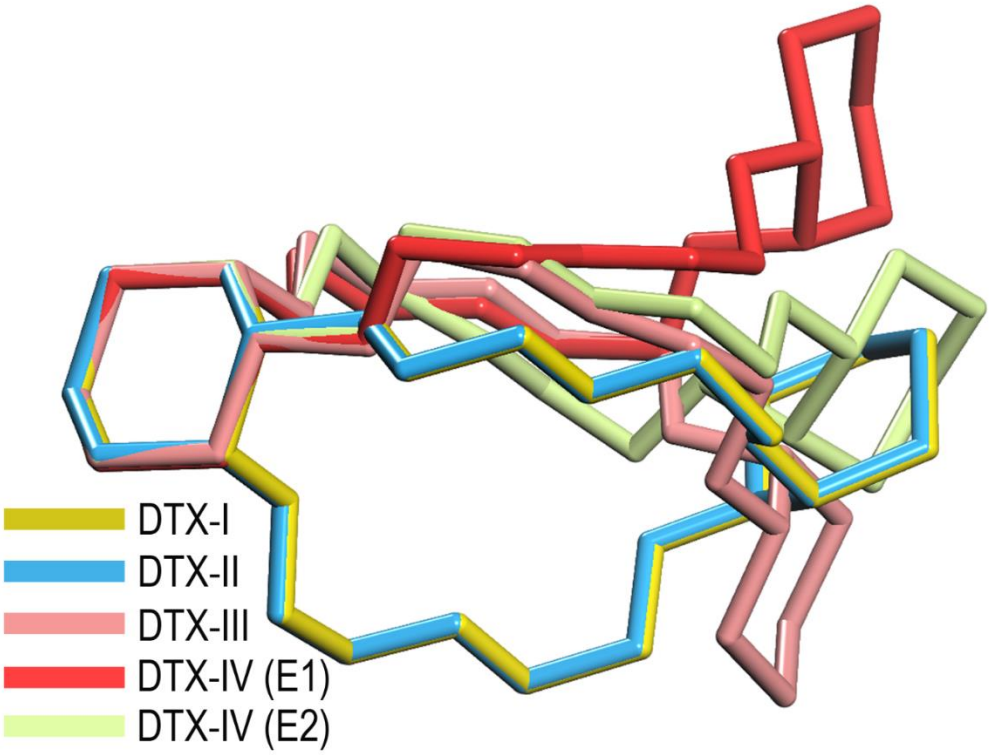

Fig. S7 Overlap images of DCH in various complexes of DTX. The distinct conformational preferences highlight the flexibility in the system that leads to the formation of complexes with varying stoichiometry and interaction types.

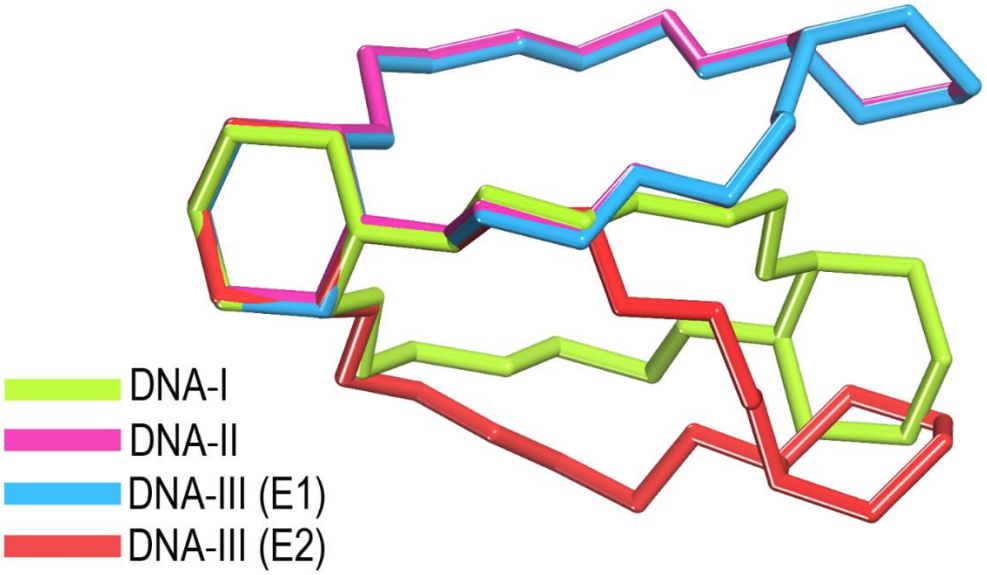

Fig. S8 Overlap images of DCH in various complexes of DNA.

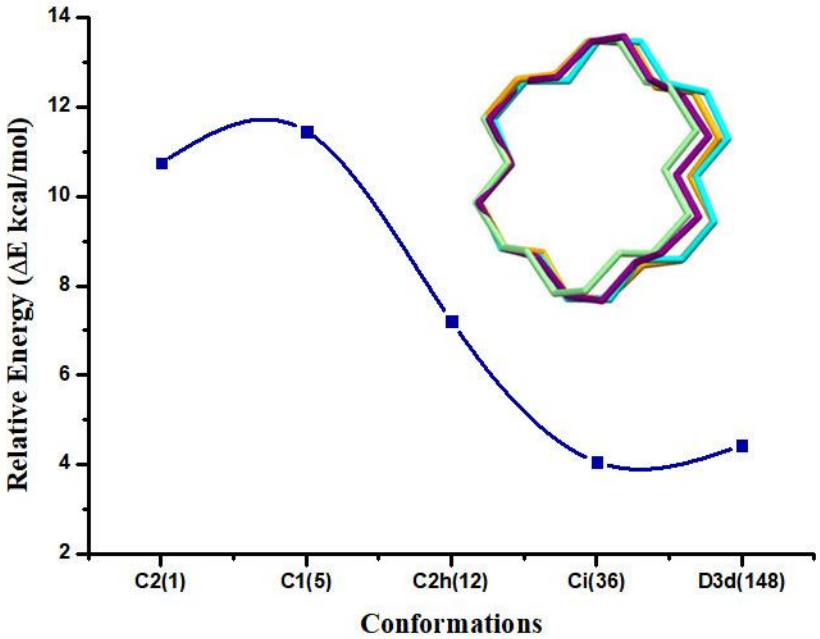

Fig. S9 Relative energy of various known conformations of 18C6. The numbers in brackets indicate the frequency distribution of various conformations. Structure overlay of several conformations is depicted in the figure. Colour code: Orange- D_{3d}, Light Green- C_i, Cyan- C_{2h}, Purple- C_1.

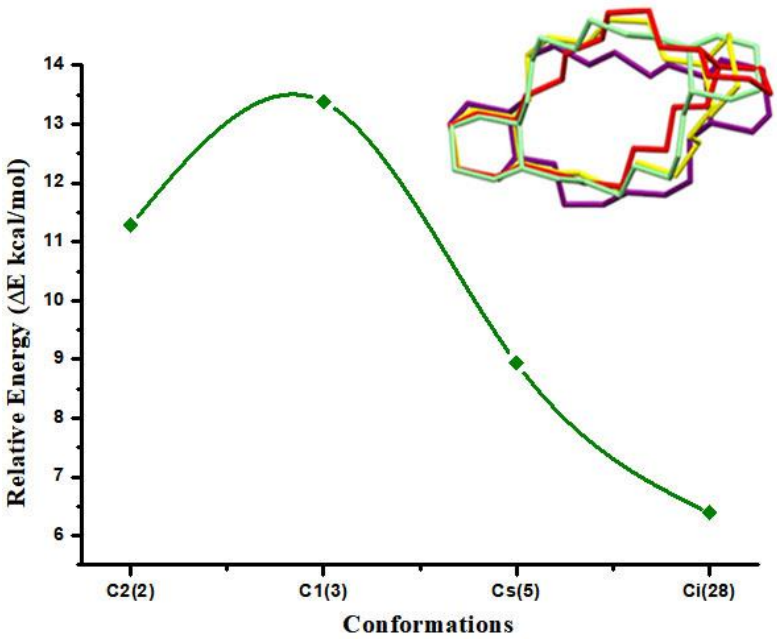

Fig. S10 Relative energy of various known conformations of DCH. The numbers in brackets indicate the frequency distributions of various conformations. Structure overlay of several conformations is depicted in the figure. Colour code: Light Green- C_i, Violet- C_s, Purple- C_1, Yellow- C_2.

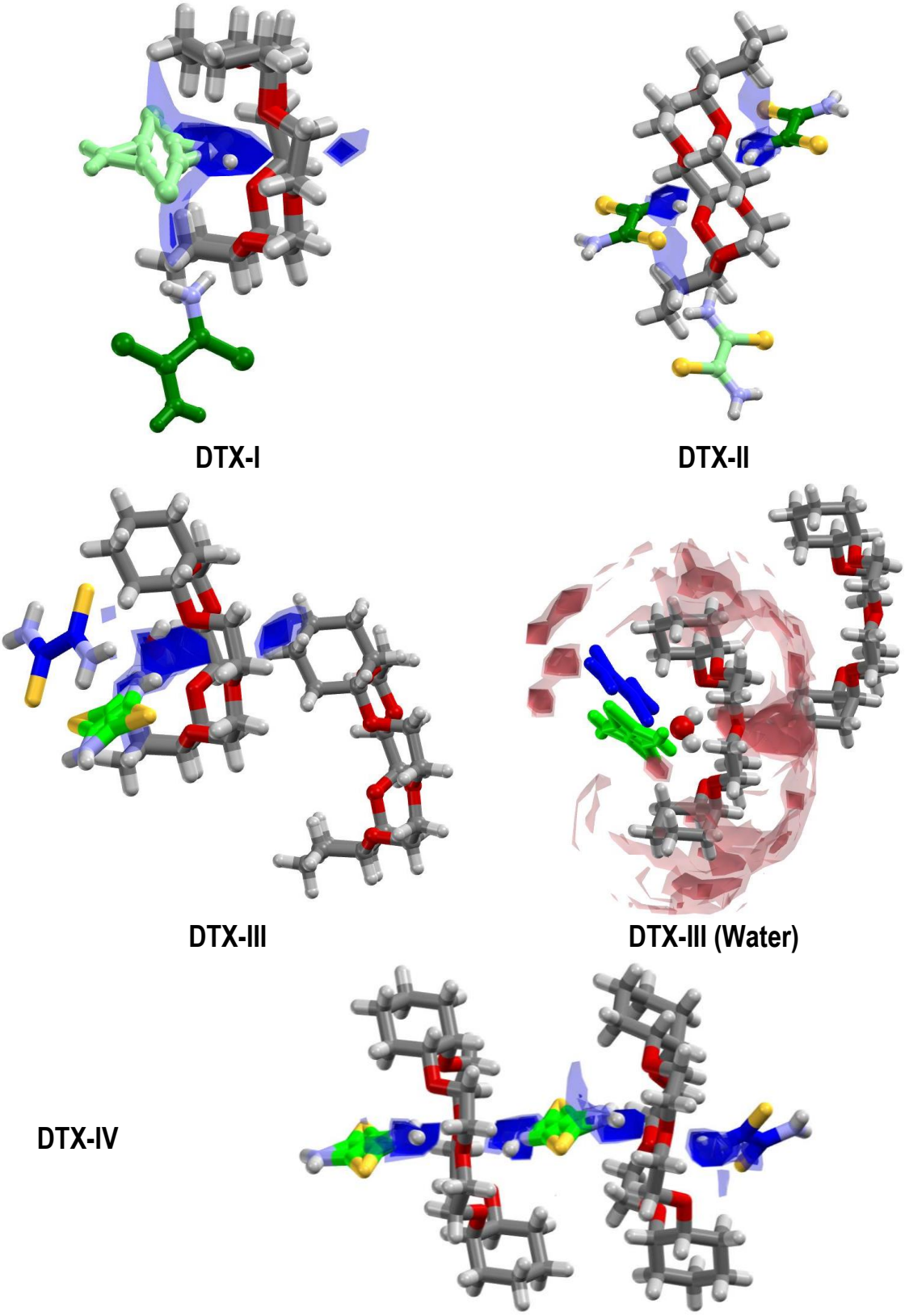

Fig. S10 The Full Interaction Maps calculated for DTX I – IV. (Symmetry-independent DTX molecules are highlighted in distinct colours)

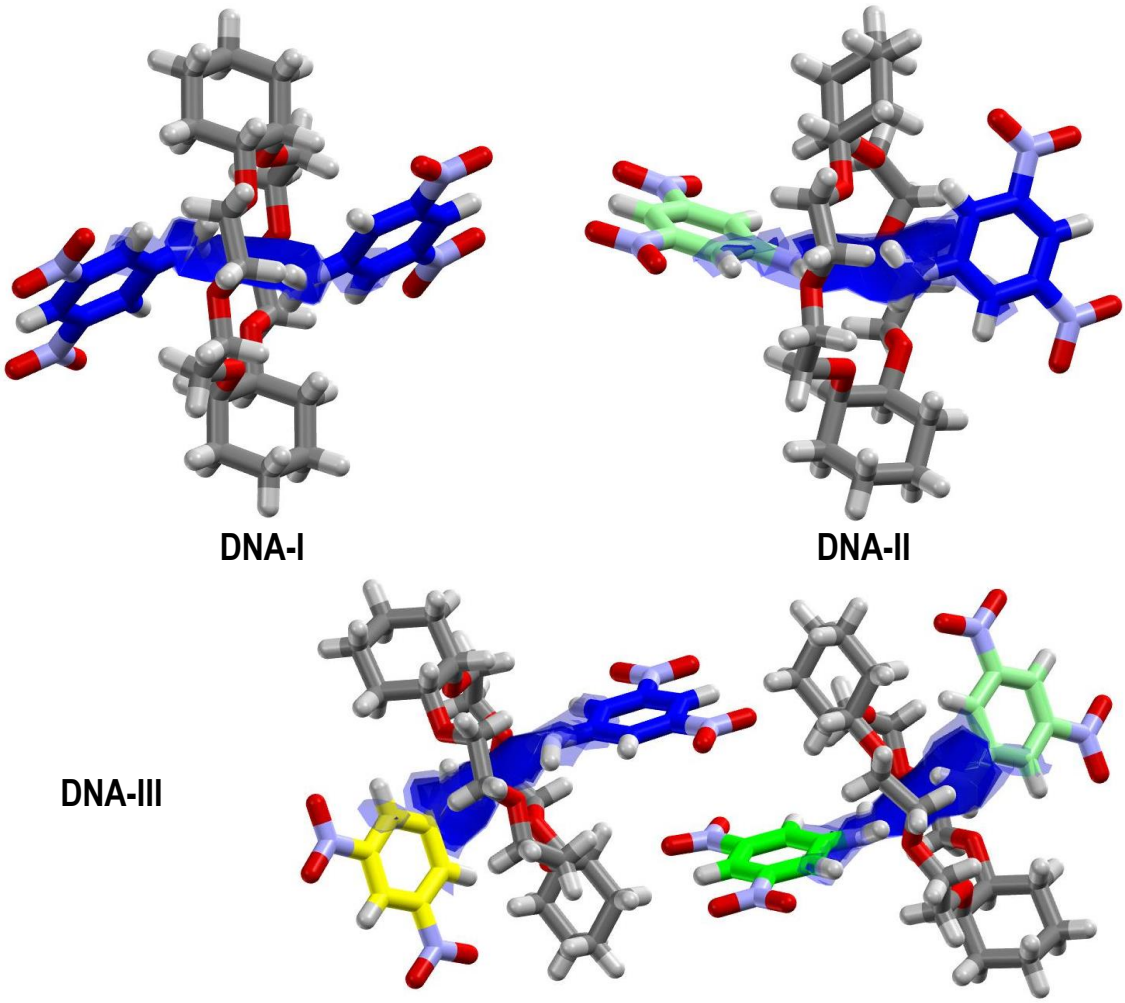

Fig. S11 The Full Interaction Maps calculated for DNA I – III. (Symmetry-independent DNA molecules are highlighted in distinct colours)

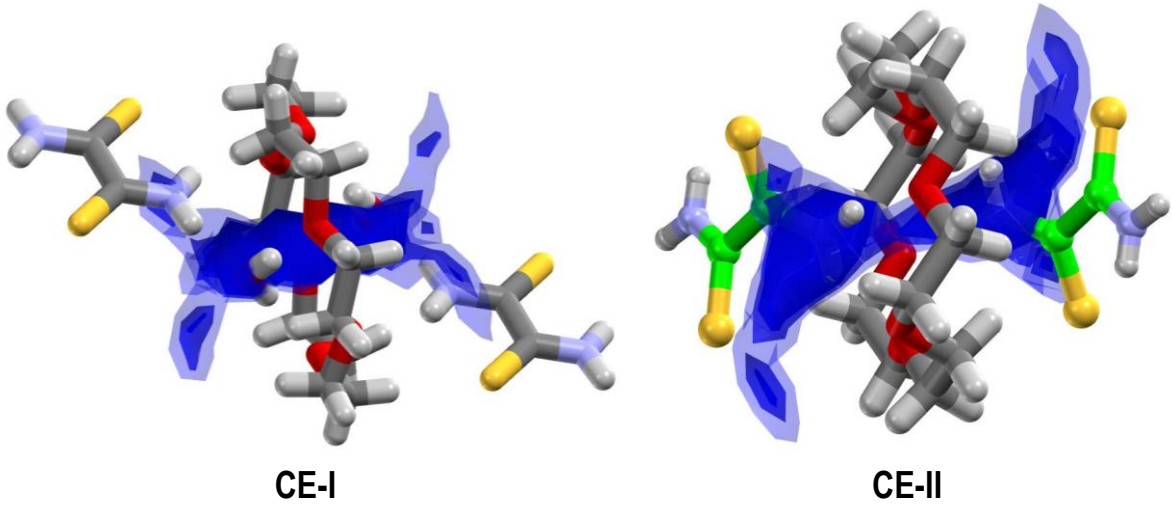

Fig. S12 The Full Interaction Maps calculated for CE-I and CE-II

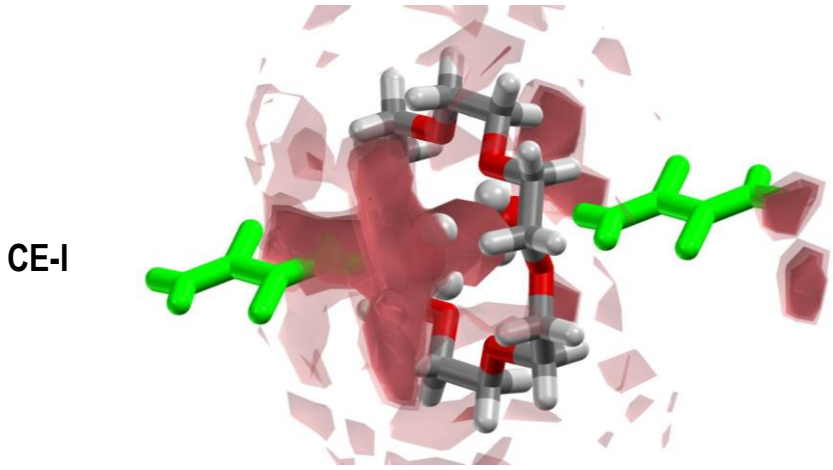

Fig. S13 The Full Interaction Maps calculated for the crown ether with respect to the lattice water in CE-I.

Complex	Point Group	Conformation and symmetry elements
DTX-I	*C2*	*cis-syn-cis* 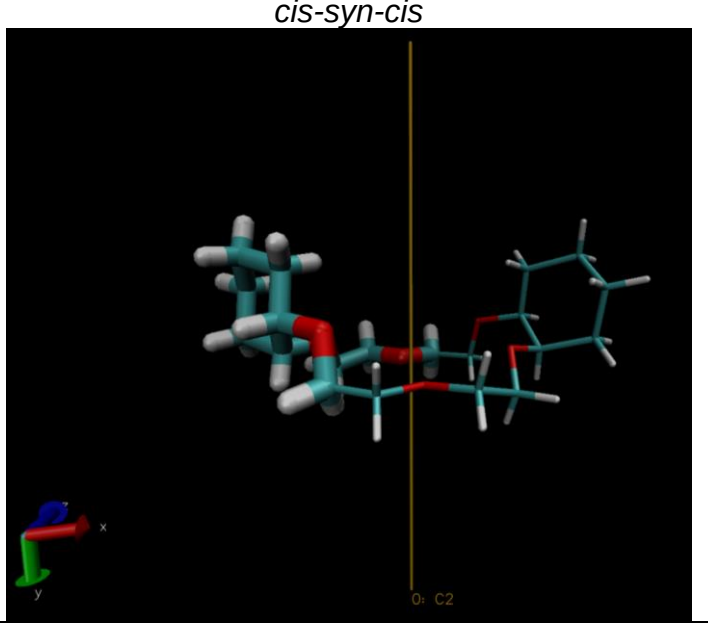
DTX-II	*Ci*	*cis-anti-cis* 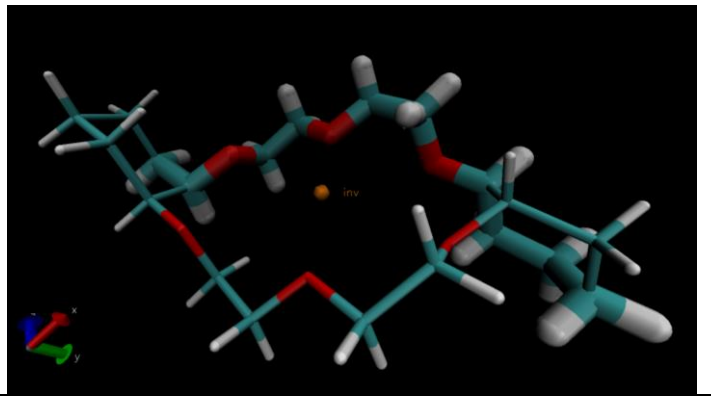
DTX-III	*Cs*	*cis-syn-cis*

		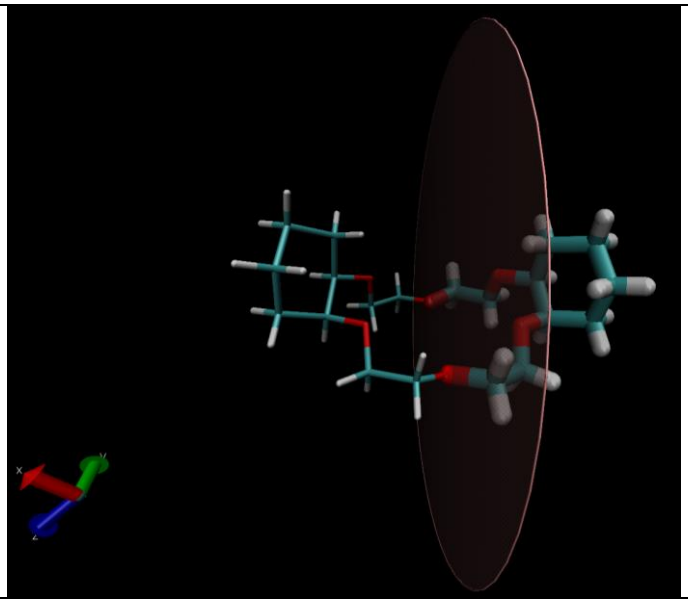
		cis-anti-cis
DTX-IV	*C1*	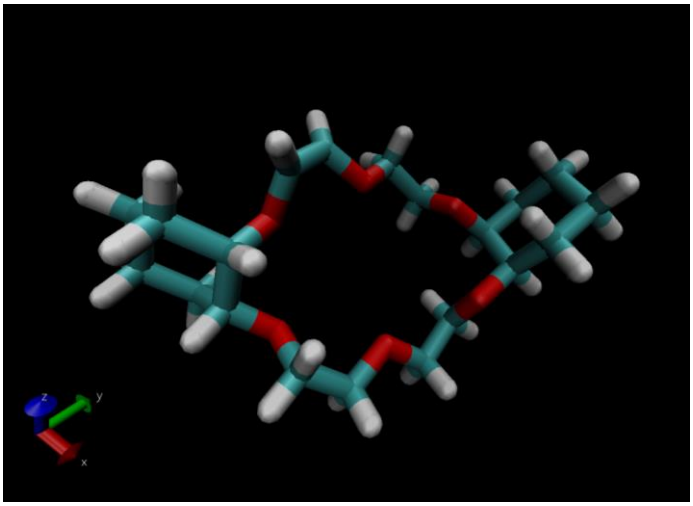
		cis-anti-cis
	Ci	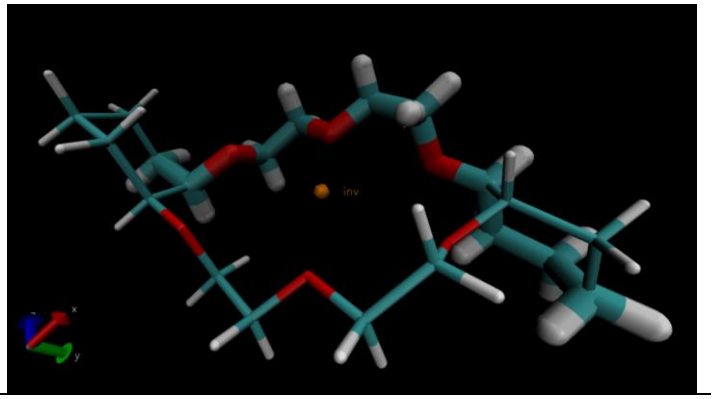
DNA-I	*Ci*	*cis-anti-cis*

		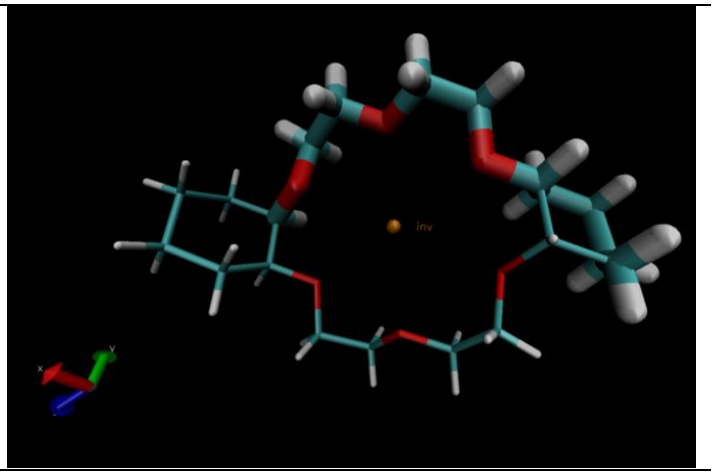
		cis-syn-cis
DNA-II	*C1*	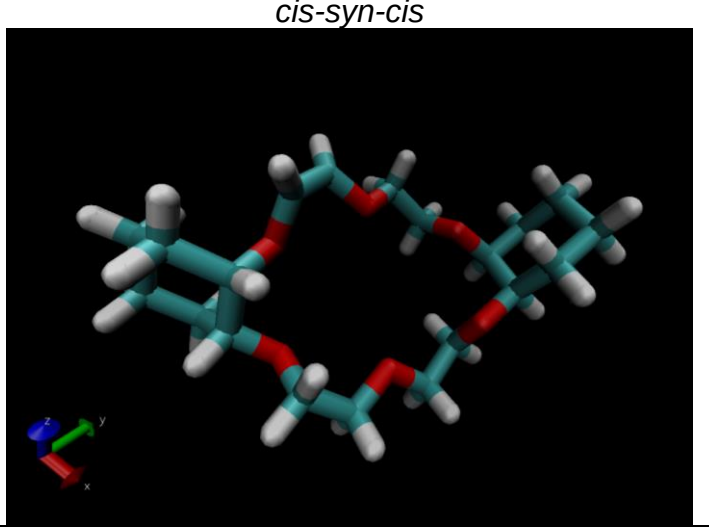
		cis-syn-cis
DNA-III	*C1*	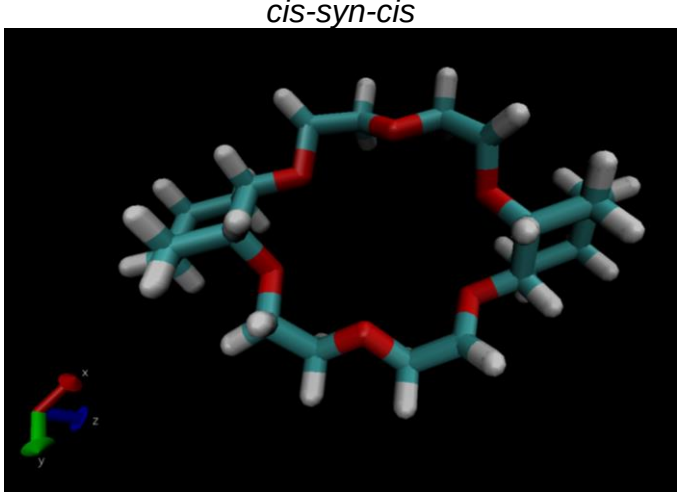
	C1	*cis-syn-cis*

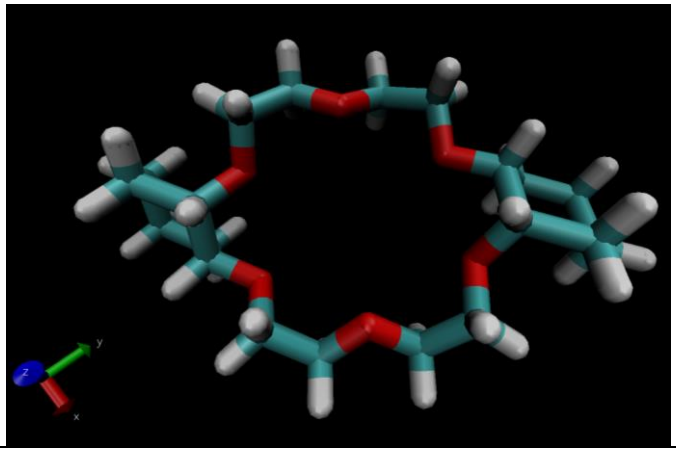

Fig. S14 The point groups, conformations and the corresponding symmetry elements adopted by the DCH moiety in its complexes. The unique structural fragment is thickened for easy identification

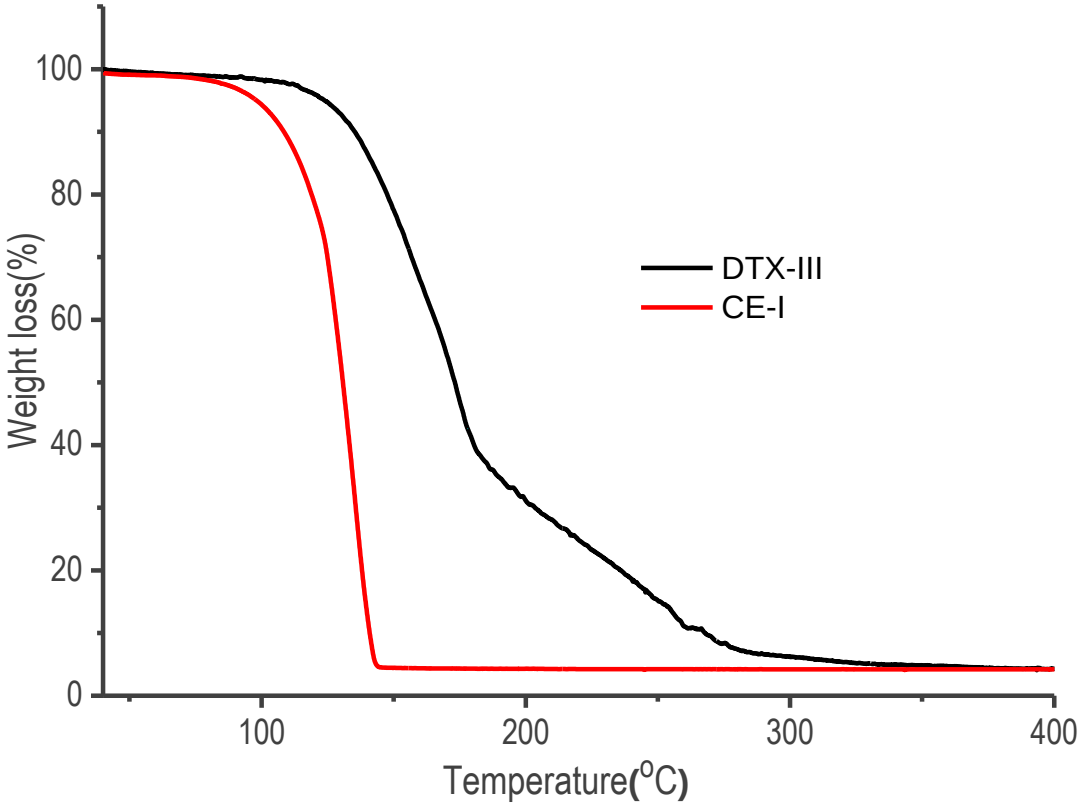

Fig. S15 The TG thermograms of the hydrated complexes DTX-III and CE-I. It is evident that the loss of the crystal water leads to the dissociation and decomposition of the complexes, highlighting the significance of the water and its interactions in the formation of the complexes.

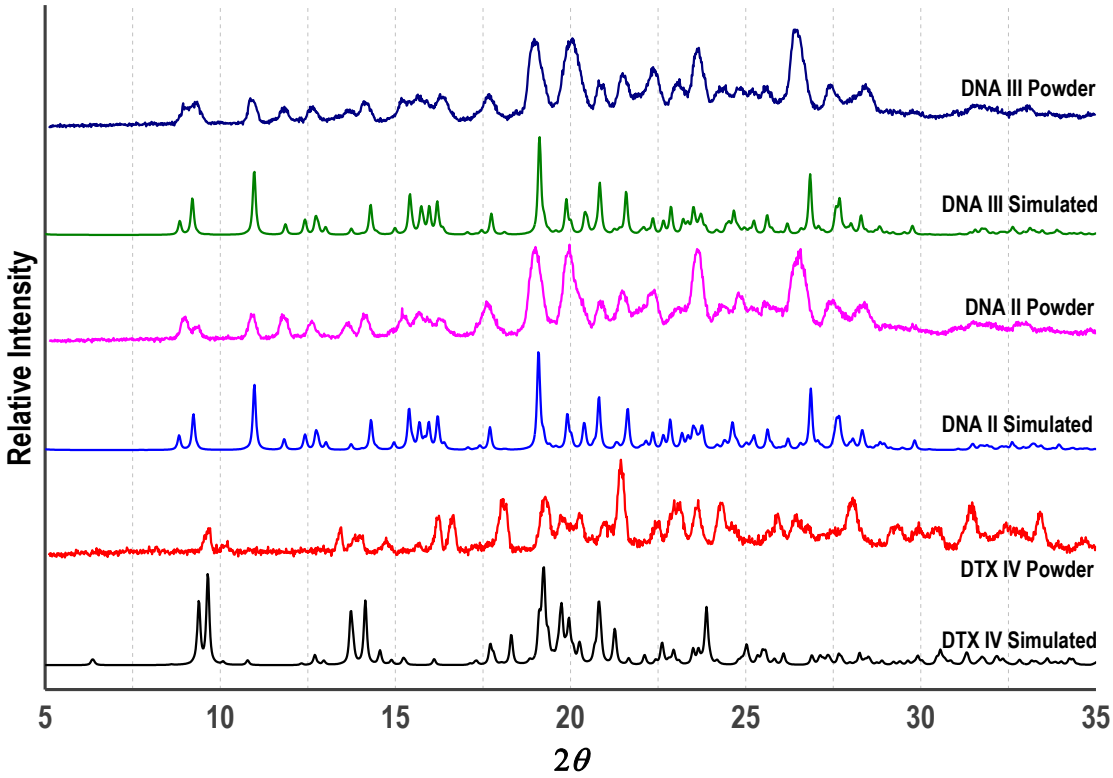

Fig. S16 The scalability and reproducibility of the complexes were explored by the mechanochemical methods. The powder patterns obtained are identical to the simulated patterns.